

# Shock Induced Particle Curtain Dispersion: Asymptotic Drag Law Scaling Formulations and Relationship to Streamwise Pressure Difference Models

Lawrence DeChant<sup>1</sup>, Kyle Daniel<sup>2</sup>, Justin Wagner<sup>3</sup>, Russ Teeter<sup>4</sup>  
*Sandia National Laboratories, Albuquerque, NM, 87185-0825*

**[Abstract]** Here we examine models for particle curtain dispersion using drag based formalisms and their connection to streamwise pressure difference closures. Focusing on drag models, we specifically demonstrate that scaling arguments developed in DeMauro et. al. [1] using early time drag modeling can be extended to include late time particle curtain dispersion behavior by weighting the dynamic portion of the drag relative velocity e.g.

$(U - \frac{dx}{dt}) \rightarrow (U - \alpha \varphi^{-1/4} \frac{dx}{dt})$  by the inverse of the particle volume fraction to the  $\frac{1}{4}$ th power. The additional

parameter e.g.  $\alpha$  introduced in this scaling is related to the model drag parameters by employing an early-time late-time matching argument. Comparison with the scaled measurements of DeMauro et. al. suggest that the proposed modification is an effective formalism. Next, the connection between drag-based models and streamwise pressure difference-based expressions is explored by formulating simple analytical models that verify an empirical (Daniel and Wagner [2]) upstream-downstream expression. Though simple, these models provide physics-based approaches describing shock particle curtain interaction behavior.

## Nomenclature

$A$	= area
$c$	= constant (locally defined)
$d$	= particle diameter
$F$	= force
$M$	= Mach number
$n$	= model exponent
$p$	= pressure
$p_d$	= post shock downstream of curtain pressure
$p_u$	= post shock upstream of curtain pressure
$Re$	= Reynolds number
$t$	= time
$U$	= post shock local velocity
$u_2$	= post-shock gas velocity
$x$	= change in particle curtain width
$X$	= particle curtain $X = \delta_0 + x$
$\alpha$	= closure coefficient
$\nu$	= kinematic viscosity
$\varepsilon$	= porosity
$\gamma$	= specific heat ratio or locally defined model constant
$\delta_0$	= initial particle curtain thickness
$\varphi$	= particle curtain solid volume fraction
$\rho_1$	= pre-shock gas density
$\rho_p$	= particle density
$\rho$	= post shock gas density

<sup>1</sup> Technical Staff, Aerosciences Dept., P.O. Box 5800, MS 0825, Albuquerque, NM, 87185, Member AIAA

<sup>2</sup> Technical Staff, Aerosciences Dept., P.O. Box 5800, MS 0825, Albuquerque, NM, 87185, Member AIAA

<sup>3</sup> Technical Staff, Aerosciences Dept., P.O. Box 5800, MS 0825, Albuquerque, NM, 87185, Member AIAA

<sup>4</sup> Technical Staff, Aerosciences Dept., P.O. Box 5800, MS 0825, Albuquerque, NM, 87185, Member AIAA

Subscripts/superscripts

0 = constant or pre-orifice location  
 1 = pre-shock or orifice location  
 2 = post-shock or post orifice location  
 ave = average  
 early = asymptotic early time  
 late = asymptotic late time  
 m = match

## I. Introduction

Dispersion of particles by shock interaction is a fundamental problem in multi-phase shock physics with numerous relevant applications as described in [1]. While high fidelity computational efforts and experimental measurements are capable of providing detailed shock dispersion behavior a simple analytical approach is valuable for preliminary design applications and as a way to delineate relevant physical behavior. A series of simple analytical arguments combined with detailed physical measurements were used by DeMauro et. al. [1] to analyze particle curtain dispersion due to moving shock interaction. In that study a particle volume fraction scaling argument was justified by examining simple Lagrangian particle behavior with appropriate drag force constant calibration valid for early time interaction. Comparison with data suggested that this choice of variable is an effective description of the volume fraction behavior for the dispersion process. Moreover, this scaling law appears to be effective well beyond the theoretically justified early time behavior. As such, we examine the efficacy and justification needed to extend the simple early time argument to asymptotic late time behavior. The resulting modifications are discussed here using both physical and mathematical closure arguments. We emphasize that no additional parameters are introduced in our expressions beyond the tradition drag formulation.

Local particle drag models provide a relevant force closure model for both individual particles and the particle curtain, however other approaches are known. For example, an upstream-downstream pressure difference model,

analogous to the pressure drop over a screen:  $\varphi \rho_p \delta_0 A \frac{d^2 x}{dt^2} = F_p \propto \varphi A (p_u - p_d)$  provides another loading expression.

Here we examine the physical basis of this approach using simple analytical models to better elucidate physical behavior. A particularly relevant description of this problem is provided by Daniel and Wagner [2] who discuss analysis and measurements for the shock-particle interaction problem. An empirical result from that study suggests that the pressure difference that causes dispersion of the associated with the particle curtain can be described by:

$$p_u - p_d = C_{meas} \varphi^{1/2} \rho_1 u_2^2 \quad ; \quad C_{meas} = 9.6 \quad (1)$$

Measurements from Daniel and Wagner demonstrate the efficacy of equation (1). Using a screen drag pressure drop model as a surrogate for the particle curtain with appropriate extensions for compressible flow behavior we can show good agreement with the Daniel and Wagner [2] result.

While useful in terms of providing simple analytical tools, the construction of these models using both drag formalisms and stream pressure balance also permit us to examine the component physical processes inherent to the multiphase shock particle curtain interaction. We examine the drag-based scaling formulation and the pressure difference formulations in detail.

## II. Early-Late Time Asymptotic Drag-Based Models

Consideration of the force balance using the drag-based formalism of DeMauro et. a. [1] on a unit area segment of the particle curtain starts with:

$$\varphi \rho_p \delta_0 \frac{d^2 x}{dt^2} = \rho \left( \alpha_1 \frac{v}{d} + \alpha_2 (U - \frac{dx}{dt}) \right) (U - \frac{dx}{dt}) \quad (2)$$

Where the two “constants”  $\alpha_1$  and  $\alpha_2$  describe a low Reynolds number and high Reynolds number drag laws, respectively. These so-called “constant” expressions contain other information including volume fraction or Reynolds number information. Indeed, they must allow for the fact that for  $\varphi \ll 1$  that the particle displacement must also be negligible. If this limit is to be bounded, we expect that  $\alpha_1 \propto \varphi^{n_1}$ ;  $n_1 > 1$  and  $\alpha_2 \propto \varphi^{n_2}$ ;  $n_2 > 1$ . Indeed, in the analytical work developed in [1] we proposed that  $\alpha_1 \propto \alpha_2 \propto \frac{\varphi^{3/2}}{(1-\varphi)^2} \approx \varphi^{3/2}$ . The other variables are defined by:

The obvious non-dimensionalization follows as:

$$t^{**} = \frac{U}{\delta_0} t \quad ; \quad x^* = \frac{x}{\delta_0} \quad (3)$$

While  $x^* = \frac{x}{\delta_0}$  Applying these expressions to equation (2) gives:

$$\frac{d^2 x^*}{dt^{**2}} = \varphi^{1/2} \left( \frac{\rho}{\rho_p} \right) \left( C_1 \text{Re}_d^{-1} + C_2 \left( 1 - \frac{dx^*}{dt^{**}} \right) \right) \left( 1 - \frac{dx^*}{dt^{**}} \right) \quad (4)$$

where  $\text{Re}_d \equiv \frac{Ud}{\nu}$ . We emphasize the physical curtain width is  $X = \delta_0 + x \rightarrow X^* = 1 + x^* = 1 + \frac{x}{\delta_0}$

Examination of the equation (4) indicates that the magnitude of the drag source term for the particle cloud is related to the particle volume fraction  $\varphi^{1/2}$ . However, this description is incomplete since the rate of change of the drag is controlled by the relative velocity terms e.g.  $\left( 1 - \frac{dx^*}{dt^{**}} \right)$  as well. Here we propose that these relative velocity terms are also affected by particle volume fraction. Indeed, for a small particle volume fraction, we expect that the particle cloud dispersion velocity  $\frac{dx^*}{dt^{**}}$  is enhanced since particle curtain is readily penetrated and exposed to shock field. As such, a modification of the form:

$$\left( 1 - \frac{dx^*}{dt^{**}} \right) \rightarrow \left( 1 - \alpha \varphi^{-a} \frac{dx^*}{dt^{**}} \right) \quad (5)$$

would seem appropriate. We need to estimate the power law coefficient “a” and the constant  $\alpha$ .

An estimate for the power law exponent  $\alpha$  is readily obtained by noting that the drag term must be valid as  $\varphi \rightarrow 0$ . Thus, collecting the highest order terms in  $\varphi$  yields the requirement:  $2a \leq 1/2 \rightarrow a \leq 1/4$ . Thus, choosing the largest possible exponent, we select  $a = 1/4$ . The constant  $\alpha$  is estimated subsequently.

Upon choosing the drag velocity exponent equation (4) can be rewritten as:

$$\frac{d^2x^*}{dt^{*2}} = \left( c_1 + c_2 (1 - \alpha^{-1} \frac{dx^*}{dt^{**}}) \right) (1 - \alpha^{-1} \frac{dx^*}{dt^{**}}) \quad (6)$$

where  $c_1 \equiv \left( \frac{\rho}{\rho_p} \right) \text{Re}_d^{-1} C_1$  and  $c_2 \equiv \left( \frac{\rho}{\rho_p} \right) C_2$  and  $t^* = \varphi^{1/4} t^{**} = \varphi^{1/4} \frac{U}{\delta_0} t$ . Notice that equation (5) is invariant with  $\varphi$  when placed in the scaled variable  $t^*$  which is the scaling used by DeMauro et. al. [1] for the early time modeling.

Equation (6) is immediately integrable to give:

$$x^* = \alpha t^* - \frac{\alpha}{c_2} \ln \left( 1 - \frac{c_2}{c_1} (1 - \exp(-\frac{c_1}{\alpha} t^*)) \right) \quad (7)$$

Where  $c_1 \equiv \left( \frac{\rho}{\rho_p} \right) \text{Re}_d^{-1} C_1$  and  $c_2 \equiv \left( \frac{\rho}{\rho_p} \right) C_2$

Examination of equation (7) suggests that there two behaviors:

1. an early time condition and
2. a late time asymptotic behavior.

Let's examine these conditions in detail. The early time i.e.  $t^* \ll 1$  trajectory can be written:

$$x_{\text{early}}^* = \frac{1}{2} (c_1 + c_2) t^{*2} + \dots \quad (8)$$

Which reflects an approximate form of the differential equation of the form:

$$\frac{d^2 x_{\text{early}}^*}{dt^{*2}} \approx (c_1 + c_2) \quad (9)$$

Implying that the curvature is related to the dimensionless constants  $c_1$  and  $c_2$ . Notice that equation (9) is independent of the volume fraction when written in terms of  $t^* = \varphi^{1/4} t^{**}$  and does not depend on the introduce constant  $\alpha$ . We emphasize, that the constants  $c_1$  and  $c_2$  are related to the drag modeling and can be estimated by considering any one of a wide range of empirical or semi-empirical modeling parameter calibration.

In a similar manner the late time (asymptotic) result can be written

$$x_{\text{late}}^* = \alpha t^* + b \quad (10)$$

where  $b$  is the y intercept.

While, the one can more easily utilize the near field behavior to provide information for  $c_1$  and  $c_2$ , the magnitude of the associated constant  $\alpha$  is not as readily achievable. Let's examine estimates for this term. Demanding that the slopes of the near field and late time solutions match for time  $t_m^*$  gives:

$$(c_1 + c_2) t_m^* = \alpha \rightarrow t_m^* = \frac{\alpha}{c_1 + c_2} \quad (11)$$

A match of the function then gives:

$$\frac{1}{2}(c_1 + c_2)t_m^{*2} = \alpha t_m^* + b \quad (12)$$

Obviously, to proceed we need to estimate  $b$ . Here recognize that the “x” intercept say  $t_i^*$  such that  $0 = \alpha t_i^* + b \rightarrow b = -\alpha t_i^*$  associated of the linear problem is bounded between 0 and  $t_m^*$ . Actually, we have more information. The data clearly illustrate that there is a lag period where there is no spreading i.e.  $x^* = 0$  such that  $t_{lag}^* \approx 3$ . Thus, we can posit that  $3 < t_i^* < t_m^*$ . With these bounds, we can estimate that an average based on these values (we discuss the actual average subsequently) would be a good approximation for  $t_i^*$ . Let's combine these results to give a single expression for  $\alpha$ :

$$\frac{1}{2}(c_1 + c_2) \left( \frac{\alpha}{c_1 + c_2} \right)^2 = \alpha \left( \frac{\alpha}{c_1 + c_2} \right) - \alpha t_i^* \rightarrow 0 = \frac{1}{2} \alpha - (c_1 + c_2) t_i^* \quad (13)$$

To use equation (13) we need to estimate  $t_i^*$ . Let's consider three average definitions: arithmetic, harmonic and geometric:

$$t_{i\_a}^* = \frac{1}{2} \left( 3 + \frac{\alpha}{c_1 + c_2} \right) \quad ; \quad t_{i\_h}^* = \frac{2}{3^{-1} + \frac{c_1 + c_2}{\alpha}} \quad ; \quad t_{i\_g}^* = \left( 3 \frac{\alpha}{c_1 + c_2} \right)^{1/2} \quad (14)$$

Substitution of the arithmetic mean is quickly shown to yield a singular result (the arithmetic mean is not independent of the linear approximations used) while the other two can be solved to give:

$$\begin{aligned} \frac{1}{2} \alpha - (c_1 + c_2) \left( \frac{2}{3^{-1} + \frac{c_1 + c_2}{\alpha}} \right) &= 0 \rightarrow \alpha = 9(c_1 + c_2) \\ \frac{1}{2} \alpha - (c_1 + c_2) \left( 3 \frac{\alpha}{c_1 + c_2} \right)^{1/2} &= 0 \rightarrow \alpha = 12(c_1 + c_2) \end{aligned} \quad (15)$$

As a useful bounding value, we use  $t_i^* = 3$  to compute  $\alpha = 6(c_1 + c_2)$ . A reasonable choice for the model is to use  $\alpha = 9(c_1 + c_2)$ .

Empirically, we can estimate  $c_1 = 0.032$ ,  $c_2 = 0.041$  or if we permit  $c_1 = c_2$  then  $c_1 = c_2 = \frac{1}{4}(0.032 + 0.041) = 0.018$ . In figure 1 we compare the results of equation (7) with  $\alpha = 9(c_1 + c_2)$  and the estimates for  $c_1$  and  $c_2$  described here to a regression expression (with selected data points included) follow the data of DeMauro et. al [1]. expressed in terms of the variable  $t^* = \varphi^{1/4} \frac{U}{\delta_0} t$  for volume fractions ranging from  $9\% < \varphi < 32\%$ . The comparison between the model for the various values of for  $c_1$  and

$c_2$  is good suggesting that the proposed solution procedure is appropriate. Notice that  $\alpha = 9(c_1 + c_2) \approx 0.66$  implying that the late time particle velocity is  $\frac{dx^*}{dt^*} = \alpha$ . This statement is consistent with a post-shock velocity reduction.

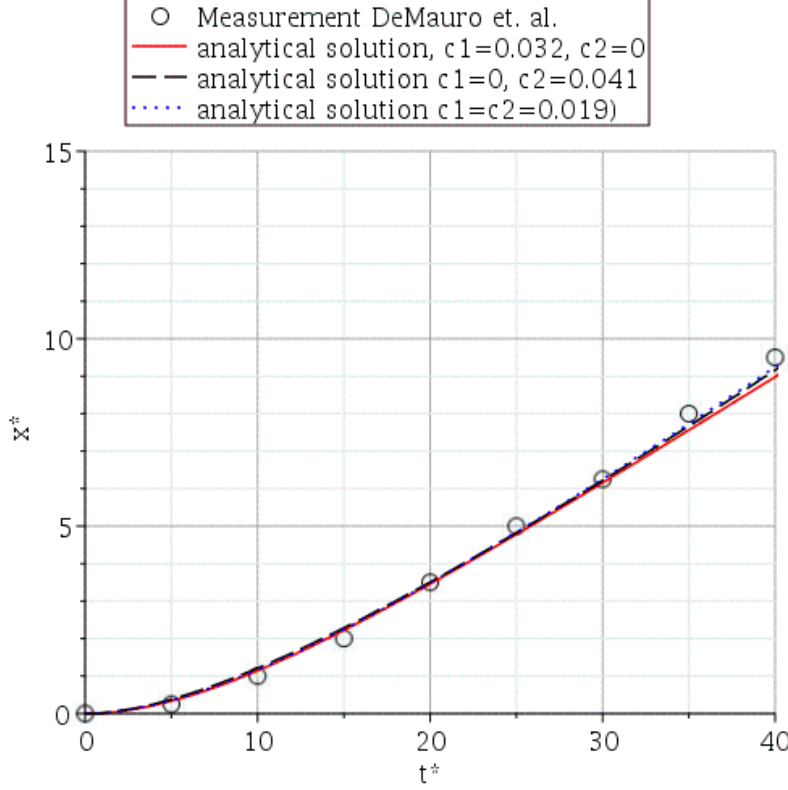


Figure 1. Comparison between equation (6) with  $\alpha = 9(c_1 + c_2)$  and the estimates for  $c_1$  and  $c_2$  and the data of DeMauro et. al. [1] suggesting that the proposed modeling approach may be generally viable.

The preceding analysis provides a useful estimate for the constants associated with drag expressions. The actual model constants,  $c_1$  and  $c_2$  we estimated by comparison with available data sets. There are approaches that can be used to estimate these constants themselves. These techniques require formulating functionally similar solutions with associated supporting parameters that are to be determined. Then, by demanding coincidence of the two functional expressions, constraint equations can be formulated that provide estimates for the associated parameters. Generally, supposition of appropriate, linearly independent functional forms that are analogous, is challenging. Here, however, there two solution immediately available corresponding to linear models (denote as  $x_l^*$ ) and quadratic models (denoted as  $x_q^*$  for the drag. We can write them as:

$$\begin{aligned} \frac{d^2 x_q^*}{dt^{*2}} &= A(1 - \alpha^{-1} \frac{dx_q^*}{dt^*})^2 \\ \frac{d^2 x_l^*}{dt^{*2}} &= B(1 - \alpha^{-1} \frac{dx_l^*}{dt^*}) \end{aligned} \tag{16}$$

Though written using the constants “A” and “B” the correspond as:  $A \approx 2c_2$  ;  $B \approx 2c_1$ . Solution to both expressions is trivial as:

$$\begin{aligned} x_q^* &= \frac{\alpha}{A} \left( At^* - \alpha \ln\left(\frac{At^* + \alpha}{\alpha}\right) \right) \\ x_l^* &= \frac{\alpha}{B} \left( Bt^* + \alpha \left( \exp\left(-\frac{B}{\alpha}t^*\right) - 1 \right) \right) \end{aligned} \quad (17)$$

Following our “prescription” we now as for equivalency between these two expressions. There are many possible constraints that we can use to achieve similar behavior. A traditional requirement, for example, is to require:  $\int_0^\infty x_q^* dt^* = \int_0^\infty x_l^* dt^*$ , unfortunately, these results are unbounded forcing us to consider other alternative. A

particularly simple constraint is to ask that the two results equal for a particular value, which is called collocation. Of course, choosing a particular value for equality is difficult, but a possible scale is  $t^* = \alpha A^{-1}$ . Using this value, we can solve the associated nonlinear expression  $x_q^*(\alpha A^{-1}) = x_l^*(\alpha A^{-1})$ . The equation can be solved exactly, but is best represented by as:  $B = 0.7840A$  since the algebra is complex. The absence of the  $\alpha$  term follows from the equation and is exact. We note that this expression is consistent with  $\frac{B}{A} = \frac{2c_1}{2c_2} \approx \frac{0.032}{0.041} = 0.781$  where we have used our empirical estimates for  $c_1$  and  $c_2$ .

Obviously, the current expression, fails to offer an explicit value for A and we need to invoke another constraint. A second viable constraint is challenging, since the collocation at a second point will yield a set of expressions with no possible solution. Indeed, one of the challenges of this approach is to identify nonlinear expressions that are non-

trivial. A constraint that is readily available and is bounded for  $t^* \gg 1$  is the acceleration  $\frac{d^2 x^*}{dt^{*2}}$ . Thus, a particularly useful constraint is to require matching at a point (say  $t^* = T^*$ ) as  $\frac{d^2 x_q^*}{dt^{*2}} \Big|_{t^* = T^*} = \frac{d^2 x_l^*}{dt^{*2}} \Big|_{t^* = T^*}$ . As before,

we need to choose an appropriate estimate for the match point. An obvious choice is simply,  $t^* = \alpha A^{-1}$ . Unfortunately, utilization of this time scale does not yield a solution, since the closure is not sufficiently independent of our previous analysis. We could alternatively, choose a different scale say,  $t^* = \alpha A^{-2}$ . This approach is viable and indeed, we can solve for an explicit value of A. A more general approach is to examine a range of closures such as:  $t^* = \alpha A^{-\gamma}$  where  $\gamma = 1/2, 1, 3/2, 2, \dots$ . We present these results in table 1.

Time scale coefficient	Solution A	$c_2 \approx A/2$
$\gamma = 1/2$	0	0
$\gamma = 1$	0	0
$\gamma = 3/2$	0.0789	0.0394
$\gamma = 2$	0.2808	0.1404

Table 1. Estimates for model coefficient for several time scale closures (collocation locations).

Examination of the  $c_2$  parameter estimate for  $\gamma=3/2$  in table 1 i.e.  $c_2 \approx A/2 \approx 0.0394$  and  $c_1 = 0.781(0.0394) = 0.0308$  as compared with the empirical result obtained previous:  $c_1 = 0.032$  and  $c_2 = 0.041$  demonstrates good agreement, suggesting that the parameter estimates are likely reasonable.

With access to the closure constants described previously, there is value in rewriting equation (5) in dimensional form. Using the previous definitions, we write:

$$\begin{aligned} \varphi \delta_0 \frac{d^2 x}{dt^2} &= \varphi U^2 \left( \varphi^{1/4} c_1 + c_2 \left( \varphi^{1/4} - \frac{1}{9(c_1 + c_2)} \frac{1}{U} \frac{dx}{dt} \right) \right) \left( \varphi^{1/4} - \frac{1}{9(c_1 + c_2)} \frac{1}{U} \frac{dx}{dt} \right) \\ &= \varphi U^2 \left( \varphi^{1/4} \left( \frac{\rho}{\rho_p} \right) \text{Re}_d^{-1} C_1 + \left( \frac{\rho}{\rho_p} \right) C_2 \left( \varphi^{1/4} - \frac{1}{9(c_1 + c_2)} \frac{1}{U} \frac{dx}{dt} \right) \right) \left( \varphi^{1/4} - \frac{1}{9(c_1 + c_2)} \frac{1}{U} \frac{dx}{dt} \right) \end{aligned} \quad (18)$$

The definitions in second line of equation (17) are useful since the gas to solid particle ratio is explicitly included.

Since the model was derived for an air soda glass problem we can estimate:  $\left( \frac{\rho}{\rho_p} \right) = O(10^{-3})$  so that the constants in equation (17) are:  $\text{Re}_d^{-1} C_1 \approx O(10^3)0.032 = 32$  and  $C_2 \approx O(10^3)c_2 = O(10^3)0.041 = 41$  implying that:

$$\varphi \delta_0 \frac{d^2 x}{dt^2} = \varphi U^2 \left( \frac{\rho}{\rho_p} \right) \left( 32\varphi^{1/4} + 41(\varphi^{1/4} - 1.52 \frac{1}{U} \frac{dx}{dt}) \right) \left( \varphi^{1/4} - 1.52 \frac{1}{U} \frac{dx}{dt} \right) \quad (19)$$

Equation (19) provides a reasonable estimate for a drag law closure. Notice that the late time particle curtain velocity is given by:  $\frac{dx}{dt} = 0.66\varphi^{1/4}U$ .

### III. Streamwise Pressure Difference Shock Particle Curtain Dispersion Models

As described previously, an upstream-downstream pressure difference model, analogous to the pressure drop over a screen which provides a formulation for the force loading dynamics of particle curtain that is more directly applied to the particle curtain as whole as compared to the drag-based formulation. A particularly relevant description of this problem is provided by Daniel and Wagner [2] who discuss analysis and measurements for the shock-particle interaction problem. An empirical result (equation (1)) from that study suggests that the pressure difference that causes dispersion of the associated with the particle curtain can be described by repeated as equation (20)):

$$p_u - p_d = C_{\text{meas}} \varphi^{1/2} \rho u_2^2 \quad ; \quad C_{\text{meas}} = 9.6 \quad (20)$$

Measurements from Daniel and Wagner demonstrate the efficacy of equation (1). Notice that this pressure gradient is directly utilized in a particle curtain drag formulation of the form:  $\varphi \rho_p \delta_0 A \frac{d^2 x}{dt^2} = F_p \propto \varphi A (p_u - p_d)$  and that a volume fraction weighting term is externally included in the right-hand-side of the force balance model.

While useful as written, there is value in ascertaining the connection between the empirical closure for equation (1) and classical theory. A successful analogy between particle curtain behavior and pressure drop associated with compressible flow over screens (wire mesh gauzes) was utilized by DeMauro et. al. [1]. In that effort, particle volume fraction behavior for the drag/pressure drop associated with particle curtain was ascertained by examination of several closures discussed by Pinker and Herbert [3] and was shown to provide a useful scaling behavior for curtain particle trajectories. However, DeMauro et. al. did not seek to ascertain the magnitude of the pressure difference, which is required to assess the empirical constant in equation (1).

Pinker and Herbert examine a range of closure models for incompressible pressure drop associated with wire gauzes to write the expression:

$$\Delta p = \frac{1}{2} \lambda_0 \rho_2 u_2^2 \quad ; \quad \lambda_0 = \lambda_0(\varphi) \quad (21)$$

Where the incompressible function  $\lambda_0(\varphi)$  is given by a range of models such as:

$$\lambda_0(\varphi) \approx c_0 \frac{1 - \varepsilon^2}{\varepsilon} = c_0 \frac{(2 - \varphi)\varphi}{(1 - \varphi)^2} \quad ; \quad c_0 \approx 0.5 \quad (22)$$

A particularly convenient representation of the volume fraction expression  $\frac{\varphi(2 - \varphi)}{(1 - \varphi)^2}$  written for  $0 < \varphi < 0.5$  can be determined using:

$$const \int_0^{0.5} \varphi^{3/2} d\varphi = \int_0^{0.5} \frac{\varphi(2 - \varphi)}{(1 - \varphi)^2} d\varphi \rightarrow const = 5\sqrt{2} \approx 7 \quad (23)$$

such that we can write:  $\lambda_0(\varphi) \approx 3.5\varphi^{3/2}$

While the pressure drop relationships described previously are viable for low-speed flow, the problem class of interest is decidedly compressible, and indeed, Pinker and Herbert describe extensions to the model to account for the increase in drag associated with compressible behavior. The behavior for compressible flow is rather more complex due to the potential for choked flow behavior. Indeed, for choked behavior one can observe a dramatic increase in the associated pressure drop. Local choking is driven by the particle curtain geometry with an increase in likelihood of choked behavior for  $\varphi \rightarrow 1$  and for higher speed behavior in the local flow field  $M_0 \rightarrow 1$ . We emphasize that  $M_0$  is the upstream of the screen/mesh/particle curtain and that  $M^* = M_0$  when the flow chokes in the mesh/particle curtain.

Pinker and Herbert [3] and [4] discuss the pressure drop (drag) for compressible flows through screens. As indicated, this process is a function of the local Mach number and particle volume fraction. The compressibility enhancement factor for  $C_{drag}$  is modeled via:

$$\frac{C_{drag}}{C_{drag\_inc}} = \left( \frac{M^*}{M^* - M_0} \right)^b \quad b \approx 1/7 \quad (24)$$

Obviously for  $M_2 \rightarrow M^*$  the pressure drop will be very large which is physically confirmed by the measurements of both [3] and [4]. To use equation (24) we need to be able to estimate the choking Mach number  $M^*$ . A good

approximation to  $M^*$  can be obtained using simple isentropic theory via the classical Mach number area relationship where the area ratio is a function of the particle volume fraction. This expression is simply:

$$M^* \left( \frac{2}{\gamma+1} \left( 1 + \frac{\gamma-1}{2} M^{*2} \right) \right)^{\frac{\gamma+1}{2(\gamma-1)}} = 1 - \varphi \quad (25)$$

Obviously for  $\varphi = 0$   $M^* = 1$ . Equation (11) is implicit for  $M^*$  which is inconvenient, but can be remedied by a simple approximation (valid for  $\gamma=1.4$ )  $M^* \left( \frac{2}{\gamma+1} \left( 1 + \frac{\gamma-1}{2} M^{*2} \right) \right)^{\frac{\gamma+1}{2(\gamma-1)}} \approx M^{*2/3}$  whereby we can approximate:  $M^* = (1 - \varphi)^{3/2}$ . Equation (5) then becomes:

$$\frac{C_{drag}}{C_{drag\_inc}} = \left( \frac{(1 - \varphi)^{3/2}}{(1 - \varphi)^{3/2} - M_2} \right)^b \quad b \approx 1/7 \quad (26)$$

The result of equation (26) can be presented in a plot of  $\frac{C_{drag}}{C_{drag\_inc}}$  as a function of  $M_2$  as shown in figure 2. The results demonstrate the strong increase in drag associated with choking in the particle curtain.

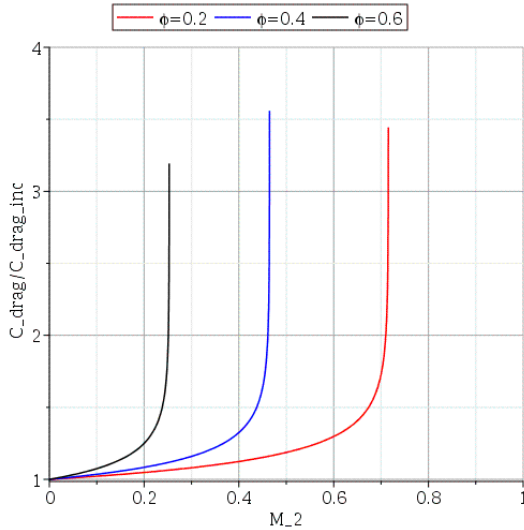


Figure 2. plot of the compressibility effect on drag  $\frac{C_{drag}}{C_{drag\_inc}}$ . Note the large increase as the Mach number approaches the choking Mach number  $M^*$

While equation (7) correctly deduces the large increase associated with choked flow, it is unfortunately not bounded, and thereby, cannot provide an upper limit for enhancement associated with the choke flow behavior. An estimate for the pressure drop across the screen choked flow is necessary.

The screen pressure drop is a characteristic of irreversible flow behaviors (weak shocks, turbulent mixing etc.) and is typically estimated empirically. A special case where analytical estimates are viable, however, is the so-called rapid expansion problem, a very well-known and classical problem associated with incompressible minor head losses. Indeed, the pressure drop (head loss) expression for the rapid expansion from a constriction area ratio:

$$\frac{A_2}{A_1} = 1 - \varphi \text{ yields } \frac{\Delta p}{\frac{1}{2} \rho u^2} = \left( \frac{A_2}{A_1} - 1 \right)^2 = \left( \frac{1}{1 - \varphi} - 1 \right)^2 = \frac{\varphi^2}{(1 - \varphi)^2} \text{ (See appendix for details.)} \text{. Further, while}$$

involved, a compressible formulation for this pressure drop is possible as well, which we derive in detail in the same appendix. Therefore, while the specific magnitude of this pressure drop model is insufficient to describe the screen drag problem, the ability to compute an analytical estimate for both compressible flow and incompressible pressure

drop and thereby provide an estimate for  $\frac{C_{drag}}{C_{drag\_inc}}$  ratio. This ratio may then in turn be used as an approximation

for a compressibility correction factor for the more general choked screen problem.

The compressible extension for the rapid expansion problem, while algebraic, does not have a closed form solution and is perhaps best examined for a range of discrete values. These values in turn support a simple regression analysis (for  $\gamma=1.4$ ) to give the simple expression:

$$\left. \frac{C_{drag}}{C_{drag\_inc}} \right|_{M^*=1} \approx 1.7 \varphi^{-4/5} \quad 0.1 < \varphi < 0.5 \quad (27)$$

We can plot the result in figure 2. Further an average value is readily obtained as:

$$\left. \frac{C_{drag}}{C_{drag\_inc}} \right|_{ave} = \frac{1.7}{1 - 0.1} \int_{0.1}^1 \varphi^{-4/5} d\varphi \approx 3.5.$$

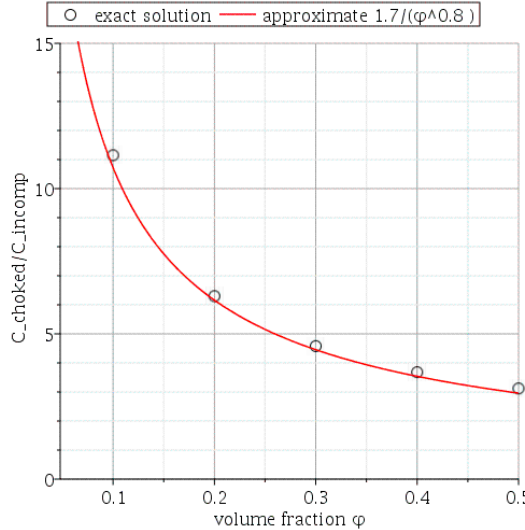


Figure 3. Comparison between exact numerical solutions and analytical approximation for  $\frac{C_{drag}}{C_{drag\_inc}}$  for rapid expansion problem.

Finally, equation (20) is based upon the pre-shock density  $\rho_1$ , whereas the formulation developed here uses the post-shock value  $\rho_2$ . The shock density ratio is computed as:

$$\frac{\rho_2}{\rho_1} = \frac{1 + \frac{\gamma+1}{\gamma-1} \left( \frac{p_2}{p_1} \right)}{\frac{\gamma+1}{\gamma-1} + \frac{p_2}{p_1}} \quad (28)$$

which can be related to the shock speed through:  $M_s^2 = \frac{\gamma+1}{2\gamma} \left( \frac{p_2}{p_1} - 1 \right) + 1$ . The measurements performed to support equation we for relatively weak shocks:  $1 < M_s < 1.7$  so that taking an integral average:  $\frac{\rho_2}{\rho_1} \Big|_{ave} = \frac{1}{1.7-1} \int_1^{1.7} \frac{\rho_2}{\rho_1} dM_s = 1.6$

Using the preceding expressions, we can then estimate the pressure difference for the particle curtain problem as described by equation (20). As a starting point we emphasize that the pressure difference for equation (20) has been weighted by  $\varphi$ , whereas the screen drag expression has not and should be directly applied without this term as:

$$\varphi \rho_p \delta_0 A \frac{d^2 x}{dt^2} = A \Delta p.$$

Let's assemble the components for the pressure difference model:

- Incompressible term:  $\lambda_0(\varphi) \approx 7c_0\varphi^{3/2} = 3.5\varphi^{3/2}$  ;  $c_0 \approx 0.5$
- Choked flow correction:  $\frac{C_{drag}}{C_{drag\_inc}} \Big|_{ave} \approx 3.5$
- Density ratio  $\frac{\rho_2}{\rho_1} \Big|_{ave} = \frac{1}{1.7-1} \int_1^{1.7} \frac{\rho_2}{\rho_1} dM_s = 1.6$

Using these expressions, we then write:

$$\Delta p = \frac{1}{2} \lambda_0(\varphi) \left( \frac{C_{drag}}{C_{drag\_inc}} \Big|_{ave} \right) \left( \frac{\rho_2}{\rho_1} \Big|_{ave} \right) \rho_1 u_2^2 = (3.5\varphi^{3/2})(3.5)(1.6)\rho_1 u_2^2 = 9.8\varphi^{3/2} \rho_1 u_2^2 \quad (29)$$

which is in good agreement with the Daniel and Wagner [2] empirical result  $C_{meas} = 9.6$ .

Obviously, there is a considerable degree of approximation inherent to the current approach and we can at best offer that the current estimates for the constants provide an order of magnitude correct value. For example, by changing the range of approximation or integration average, we could write:

- Incompressible term:  $const \int_0^{0.6} \varphi^{3/2} d\varphi = \int_0^{0.6} \frac{\varphi(2-\varphi)}{(1-\varphi)^2} d\varphi \rightarrow const \approx 8.1$  such that  $\lambda_0(\varphi) \approx 4\varphi^{3/2}$
- Choked flow correction  $\frac{C_{drag}}{C_{drag\_inc}} \Big|_{ave} = \frac{1.7}{1-0.01} \int_{0.01}^1 \varphi^{-4/5} d\varphi \approx 5.2$
- Density ratio  $\frac{\rho_2}{\rho_1} \Big|_{ave} = \frac{1}{2-1} \int_1^2 \frac{\rho_2}{\rho_1} dM_s = 1.8$

These modified values would in turn  $\Delta p = \frac{1}{2}(4\varphi^{3/2})(5.2)(1.8)\rho_1 u_2^2 = 18.7\varphi^{3/2}\rho_1 u_2^2$  larger by a factor of two as compared to the empirical result. Nonetheless, the formulation structure offers a plausible approach to support the relationship between streamwise pressure drop across the particle curtain as related to the dynamic pressure.

In summary, the modeling associated with this pressure drop closure is largely approximate but there appears to be a plausible argument to support the connection between the screen drag pressure drop models and the particle curtain behavior. More broadly, there is a supportable argument that pressure difference models and drag-based approaches are closely related.

#### IV. Conclusion

The focus of this study has been to examine particle curtain dispersion modeling approached based on drag closures and their relationship to streamwise pressure difference formulations. We specifically showed that scaling arguments developed in DeMauro et. al. [1] using early time drag modeling could be extended to include late time particle curtain dispersion behavior by weighting the dynamic portion of the drag relative velocity e.g.

$(U - \frac{dx}{dt}) \rightarrow (U - \alpha\varphi^{-1/4} \frac{dx}{dt})$  by the inverse of the particle volume fraction to the  $\frac{1}{4}$ th power. The addition of extra parameters in the formulation was estimated by employing an early-time late-time matching argument. Similarly, estimates for the drag law closure constants were estimated using a functional approximation/collocation method. Comparison with the scaled measurements of DeMauro et. al. suggest that the proposed modification is an effective formalism.

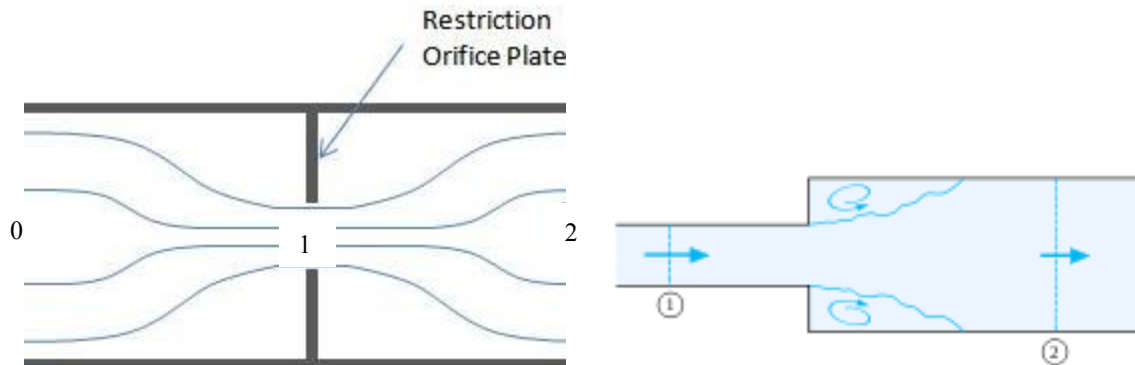
The second portion of the discussion examined the connection between drag-based models and streamwise pressure difference-based expressions. This effort involved formulating simple analytical models that verify a successful empirical (Daniel and Wagner [2]) upstream-downstream expression. Using a screen pressure drop analog, extended to include compressible flow choking effects, it was possible to directly show the relationship between classical drag and pressure difference models. Though simple, these models provide physics-based approaches describing shock particle curtain interaction behavior and help elucidate the physics associated with this complex phenomenon.

#### V. Appendix: Compressible Rapid Expansion Pressure Loss Model

Here we derive expressions describing pressure drop through a sudden expansion for compressible flow. This model is used as a surrogate for screen loss behavior, which in turn is related to particle curtain losses.

##### Incompressible Flow

Considering the plate and sudden expansion problems with the notation suggested:



we can compute the pressure drop between stations (1) and (2) using the sudden expansion approximation via the momentum equation to write the pressure drop as:

$$p_2 - p_1 = \rho u_2 (u_1 - u_2) = \rho u_0^2 \left( \frac{A_2}{A_1} - 1 \right) \quad (\text{A.1})$$

Where we have used:  $A_0 u_0 = A_1 u_1 = A_2 u_2$  ;  $A_0 = A_2$ . To eliminate the pressure at the orifice plate we assume a lossless behavior between location “0” and location “1” whereby Bernoulli’s equation and continuity give:

$$p_1 = p_0 + \frac{1}{2} \rho u_0^2 \left( 1 - \left( \frac{A_2}{A_1} \right)^2 \right) \quad (\text{A.2})$$

We can thus compute  $\frac{(p_0 - p_2)}{\frac{1}{2} \rho u_0^2} = \left( \frac{A_2}{A_1} - 1 \right)^2$  and for  $\frac{A_2}{A_1} = \frac{1}{1-\varphi}$  we have  $\frac{(p_0 - p_2)}{\frac{1}{2} \rho u_0^2} = \frac{\varphi^2}{(1-\varphi)^2}$

### Compressible Flow

The formulation for the compressible problem is broadly similar to the incompressible problem. Focusing on the irreversible portion of the flow between location “1” and “2” we write the same type of conservation formation as: mass:

$$\rho_1 u_1 A_1 = \rho_2 u_2 A_2 \quad (\text{A.3})$$

momentum:

$$\rho_1 u_1^2 A_1 + p_1 A_1 - (A_2 - A_1) p_1 = \rho_2 u_2^2 A_2 + p_2 A_2 \quad (\text{A.4})$$

and energy:

$$\rho_1 u_1 A_1 c_p T_{01} = \rho_2 u_2 A_2 c_p T_{02} \quad (\text{A.5})$$

Note, that for adiabatic flow  $T_{01} = T_{02}$  We simplify the momentum equation and then divide through by  $\rho_1 u_1^2 A_1$ .

Recognizing that (regardless of subscript) that  $\frac{p}{\rho u^2} = \frac{1}{\gamma M^2}$  we now have:

$$\left( \frac{A_2}{A_1} \right) + \gamma M_1^2 = \left( \frac{M_1^2}{M_2^2} \right) \left( \frac{u_2}{u_1} \right) \left( 1 + \gamma M_2^2 \right) \quad (\text{A.6})$$

Let’s square both sides of equation (A.6) and examine the term:  $\left( \frac{u_2}{u_1} \right)^2$ . We can relate this velocity ratio to the temperature through the Mach number definition as:

$$\frac{u_2^2}{u_1^2} = \frac{M_2^2 \gamma R T_2}{M_1^2 \gamma R T_1} = \left( \frac{M_2^2}{M_1^2} \right) \left( \frac{T_2}{T_1} \right) \quad (\text{A.7})$$

Now, we need to eliminate  $\left( \frac{T_2}{T_1} \right)$ . We use the energy equation and the total temperature definition:  
 $\frac{T_0}{T} = 1 + \frac{\gamma-1}{2} M^2$  to eliminate  $\left( \frac{T_2}{T_1} \right)$ :

$$\frac{T_2}{T_1} = \frac{1 + \frac{\gamma-1}{2} M_1^2}{1 + \frac{\gamma-1}{2} M_2^2} \left( \frac{T_{02}}{T_{01}} \right) \quad (\text{A.8})$$

Thus the velocity ratio becomes:

$$\frac{u_2^2}{u_1^2} = \left( \frac{M_2^2}{M_1^2} \right) \left( \frac{1 + \frac{\gamma-1}{2} M_1^2}{1 + \frac{\gamma-1}{2} M_2^2} \right) \left( \frac{T_{02}}{T_{01}} \right) \quad (\text{A.9})$$

So put it all together in:  $\left( \left( \frac{A_2}{A_1} \right) + \gamma M_1^2 \right)^2 = \left( \frac{M_1^2}{M_2^2} \right)^2 \left( \frac{u_2}{u_1} \right)^2 (1 + \gamma M_2^2)^2$  and collect terms to yield:

$$\frac{\left( 1 + \frac{\gamma-1}{2} M_2^2 \right) M_2^2}{(1 + \gamma M_2^2)^2} = \left( \frac{T_{02}}{T_{01}} \right) \frac{\left( 1 + \frac{\gamma-1}{2} M_1^2 \right) M_1^2}{\left( \left( \frac{A_2}{A_1} \right) + \gamma M_1^2 \right)^2} \quad (\text{A.10})$$

This expression is the same as that described in Shapiro [5]. If we ignore the heat transfer  $\frac{T_{02}}{T_{01}} = 1$ . To utilize equation (A.10) we need to estimate  $M_1$  in terms of  $M_0$ . Following the zero energy loss estimate (Bernoulli's equation) from the incompressible formulation we assume a similar isentropic model as simply write:

$$\frac{M_1}{M_0} \left( \frac{1 + \frac{\gamma-1}{2} M_0^2}{1 + \frac{\gamma-1}{2} M_1^2} \right)^{(1+\gamma)/2(\gamma-1)} = \frac{A_2}{A_1} \quad (\text{A.11})$$

Equations (10) and (11) provide a method to estimate the downstream Mach number, i.e.  $M_2$  given the passage of the flow through the orifice described by the  $\frac{A_2}{A_1}$  ratio. The next step is to compute the pressure drop for this problem.

We can use the preceding equations to compute the drag coefficient  $\frac{(p_0 - p_2)}{\frac{1}{2} \rho u_0^2} = \frac{[(p_0 - p_1) - (p_2 - p_1)]}{\frac{1}{2} \rho u_0^2}$ .

While it is possible to compute the downstream pressure  $p_2$  using the Mach number at location “2”, the total temperature and state, the result is not well posed for incompressible flow and is thus not particularly useful. An alternative formulation that more closely mimics the incompressible formula is preferred. Using the momentum equation (along with state) we compute:

$$p_1 - p_2 = \rho_1 u_1^2 \frac{A_1}{A_2} \left( \frac{u_2}{u_1} - 1 \right) \quad (\text{A.12})$$

We can express the velocity ratio in terms of the Mach numbers as:  $\frac{u_2}{u_1} = \frac{M_2}{M_1} \left( \frac{1 + \frac{\gamma-1}{2} M_1^2}{1 + \frac{\gamma-1}{2} M_2^2} \right)^{1/2}$ . Using

continuity between location “1” and location “0” we can write:  $\frac{\rho_1 u_1}{\rho_0 u_0} = \frac{A_0}{A_1} = \frac{A_2}{A_1}$  we can then write:

$$\frac{p_2 - p_1}{\frac{1}{2} \rho_0 u_0^2} = 2 \frac{M_1}{M_0} \left( \frac{1 + \frac{\gamma-1}{2} M_0^2}{1 + \frac{\gamma-1}{2} M_1^2} \right)^{1/2} \left( 1 - \frac{M_2}{M_1} \left( \frac{1 + \frac{\gamma-1}{2} M_1^2}{1 + \frac{\gamma-1}{2} M_2^2} \right)^{1/2} \right) \quad (\text{A.13})$$

The Mach number terms in this expression are specified previously. To compute the drag we also need access to  $\frac{(p_0 - p_1)}{\frac{1}{2} \rho u_0^2}$  since we will compute the drag using  $K = \frac{(p_0 - p_2)}{\frac{1}{2} \rho u_0^2} = \frac{[(p_0 - p_1) - (p_2 - p_1)]}{\frac{1}{2} \rho u_0^2}$ . Since the flow

is isentropic between location “0” and “1” so that we can write:

$$\frac{(p_0 - p_1)}{\frac{1}{2} \rho u_0^2} = \frac{p_0}{\frac{1}{2} \rho u_0^2} \left( 1 - \frac{p_1}{p_0} \right) = \frac{2}{\gamma M_0^2} \left( 1 - \left( \frac{1 + \frac{\gamma-1}{2} M_0^2}{1 + \frac{\gamma-1}{2} M_1^2} \right)^{\frac{\gamma}{\gamma-1}} \right) \quad (\text{A.14})$$

Equations (A.13) and (A.14) provide access to the pressure loss  $K$  with  $K$  defined by  $K = \text{Equ(A.14)} - \text{Equ(A.13)}$ .

Since we have derived these expressions with the idea that they will correctly recover  $M=0$  behavior we consider the limiting behavior. Equation (A.14) simplifies as:

$$\frac{(p_0 - p_1)}{\frac{1}{2} \rho u_0^2} = \left( \frac{2}{\gamma M_0^2} \right) \left( \frac{\gamma}{2} \right) (M_1^2 - M_0^2) = \left( \frac{u_1}{u_0} \right)^2 - 1 = \left( \frac{A_2}{A_1} \right)^2 - 1 \quad (\text{A.15})$$

While equation (A.13) becomes:

$$\frac{p_2 - p_1}{\frac{1}{2} \rho_0 u_0^2} = 2 \frac{u_1}{u_0} \left( 1 - \frac{u_2}{u_1} \right) \rightarrow \frac{p_2 - p_1}{\frac{1}{2} \rho_0 u_0^2} = 2 \left( \frac{A_2}{A_1} - 1 \right) \quad (\text{A.16})$$

$$\text{Thus } K_{inc} = \frac{(p_0 - p_1)}{\frac{1}{2} \rho u_0^2} \left| - \frac{(p_2 - p_1)}{\frac{1}{2} \rho u_0^2} = \left( \frac{A_2}{A_1} \right)^2 - 1 - \left[ 2 \left( \frac{A_2}{A_1} - 1 \right) \right] = \left( \frac{A_2}{A_1} - 1 \right)^2 \right. \text{ which is the expected result with}$$

An important limiting case is associated with the preceding discussion, namely, where flow in the pore system is choked, i.e.  $M_1=1$ . Under these conditions the upstream Mach number is no longer a free parameter for steady flow but is defined by equation (14) through:

$$\frac{1}{M_0} \left( \frac{2}{\gamma+1} \left( 1 + \frac{\gamma-1}{2} M_0^2 \right) \right)^{(1+\gamma)/2(\gamma-1)} = \frac{A_2}{A_1} = \frac{1}{1-\varphi} \quad (\text{A.17})$$

In a similar manner, equation (A.10) and the pressure drop expressions, i.e. equations (A.13) and (A.14) can be utilized by simply replacing  $M_1=1$ .

As stated previously, the magnitude of the current pressure drop model is of rather less importance relative to providing an estimate for the ratio of choked flow compressible pressure drop to the incompressible value i.e.

$\frac{C_{drag}}{C_{drag\_inc}}$ . This ratio is readily computed as:

$$\frac{C_{drag}}{C_{drag\_inc}} = \frac{equ(A.14)|_{M_1=1} - equ(A.13)|_{M_1=1}}{\frac{\varphi^2}{(1-\varphi)^2}} \quad (\text{A.18})$$

Equation (18) is the main result of the appendix and provides an estimate for the increase in drag associated with choked flow behavior. Note that for  $\gamma = 1.4$  (most usefully) that equation (A.18) is a (complex) function of  $\varphi$  only. This fact is leveraged to compute equation (8).

The expression provided in equation (8) in the text and equation (A.18) are useful (and correct) as written, but may be misleading. Examination of equation (8) seems to suggest that  $\frac{C_{drag}}{C_{drag\_inc}}$  is unbounded for small volume fraction  $\varphi$ . Indeed, as written, this is true, and there is value in examining why and how this behavior occurs. Let's then examine the formulation of the problem for  $\varphi \ll 1$ . We will use  $\gamma = 7/5$ . The expressions we need are

equation (A.11) with  $\frac{A_2}{A_1} = \frac{1}{1-\varphi} \rightarrow \frac{A_2}{A_1} = 1 + \varphi$  and the corresponding expression for the upstream Mach number  $M_0$  is solvable as:

$$M_0 = 1 - \frac{\sqrt{30}}{5} \varphi^{1/2} + \dots \quad (\text{A.19})$$

A similar computation is possible for equation (A.10) which yields the down stream Mach number  $M_2$  as:

$$M_2 = 1 - \frac{\sqrt{30}}{5} \varphi^{1/2} + \frac{\sqrt{30}}{16} \varphi^{3/2} + \dots \quad (\text{A.20})$$

With these solutions, the preceding for the numerator of equation (A.18) is readily solvable as:

$$C_{drag} = \text{equ}(A.14)|_{M_1=1} - \text{equ}(A.13)|_{M_1=1} = \frac{47\sqrt{30}}{144} \varphi^{3/2} + \dots \quad (\text{A.21})$$

Let's now examine the behavior for denominator, i.e. the incompressible drag for  $\varphi \ll 1$  which gives:

$$C_{drag\_inc} = \frac{\varphi^2}{(1-\varphi)^2} \approx \varphi^2 + \dots \quad (\text{A.22})$$

We immediately detect the unbounded behavior for  $\frac{C_{drag}}{C_{drag\_inc}} \Big|_{\varphi \ll 1}$  as be proportional as  $\frac{C_{drag}}{C_{drag\_inc}} \Big|_{\varphi \ll 1} \propto \varphi^{-1/2}$ ;

obviously the choked flow limit for  $\varphi \ll 1$  and the incompressible limit for  $\varphi \ll 1$  behave differently. While this behavior causes unboundedness of the ratio of the choked drag to incompressible drag for  $\varphi \ll 1$ , the actual value

(unscaled)  $C_{drag} = \frac{47\sqrt{30}}{144} \varphi^{3/2} \approx 1.8\varphi^{3/2} + \dots$  is consistent with the closure described previously:  $\lambda_0(\varphi) \propto \varphi^{3/2}$ .

## VI. Acknowledgements

Sandia National Laboratories is a multi-mission laboratory managed and operated by National Technology and Engineering Solutions of Sandia, LLC., a wholly owned subsidiary of Honeywell International, Inc., for the U.S. Department of Energy's National Nuclear Security Administration under contract DE-NA0003525.

## VII. References

1. DeMauro, E. P., Wagner, J. L., DeChant, L. J., Beresh, S. J., Turpin, A.M., "Improved Scaling Laws for Shock-Induced Dispersal of a Dense Particle Curtain," *J. of Fluid Mechanics*, V. 876, pp. 881-895, 2019.
2. Daniel, K., Wagner, J. L., "The Shock-Induced Dispersal of Particle Curtains with Varying Material Density," *Int. J. of Multiphase Flow*, V152, 104082, 2022.
3. Pinker, R. A., Herbert, M. V., Pressure Loss Associated with Compressible Flow Through Square-Mesh Wire Gauzes," *J. Mechanical Eng. Sci.*, V. 9 pp. 11-23, 1967.
4. Su, C. C., Huang, C. C., "Experimental Studies of Flow Through Single Gauzes," *Int. J. Heat and Fluid Flow*, V. 12., 3, pp. 273-278, 1991.

5. Shapiro, A. H., *The Dynamics and Thermodynamics of Compressible Fluid Flow*, Wiley, NY, 1991.